IEEE Access
Multidisciplinary ⋮ Rapid Review ⋮ Open Access Journal

Received July 25, 2016, accepted August 29, 2016, date of publication October 10, 2016, date of current version November 8, 2016.

Digital Object Identifier 10.1109/ACCESS.2016.2616165

Cooperative Sleep and Power Allocation for Energy Saving in Dense Small Cell Networks

SHIE WU, FANGFANG LIU, (Member, IEEE), ZHIMIN ZENG, AND HAILUN XIA, (Member, IEEE)
Beijing Laboratory of Advanced Information Networks, School of Information and Communication Engineering, Beijing University of Posts and Telecommunications, Beijing 100876, China

Corresponding author: H. Xia (xiahailun@bupt.edu.cn)

This work was supported in part by the Chinese National Nature Science Foundation under Grant 61271177 and in part by the Fundamental Research Funds for the Central Universities under Grant 2014ZD03-01.

ABSTRACT Energy consumption has become a crucial issue due to the large-scale deployment of small base stations (SBSs) in dense small cell networks (DSCNs). In this paper, a joint optimization problem involving sleep mode in subframes and power allocation to minimize the DSCN energy consumption while guaranteeing users' rate requirements is formulated as a mixed integer nonlinear programming. To address this problem, we propose a cooperative sleep and power allocation approach by decomposing it into two subproblems. First, we derive the optimum number of active subframes for each SBS and present a centralized heuristic coalition formation algorithm to manage SBSs to form coalitions. In such a case, SBSs can transmit data in active subframes and sleep in others. We then obtain the SBSs' optimum transmit power in the active subframes relying on a distributed price-based power allocation algorithm. System-level simulation results show that our proposed cooperative scheme can yield significant performance gains in terms of energy saving compared with the maximum power allocation and the non-cooperative power allocation (NCPA) approaches. In addition, the effects of target rates on coalition size and energy consumption are also analyzed.

INDEX TERMS Dense small cell network, energy saving, cooperative sleep, power allocation, coalition formation.

I. INTRODUCTION

It is forecasted that the global mobile data traffic will grow to 30.6 EB per month by 2020, a nearly eightfold increase over 2015 [1]. In order to meet these intense demands, the investigation of 5G for the next generation of terrestrial mobile telecommunications has been triggered [2]. Furthermore, as one of the promising solutions, deploying small cell base stations (SBSs) densely to improve spectral efficiency (SE) in an area of high data traffic density is of common concern for the 5G network [3].

However, the deployment of massive small cells also brings challenges, such as interference management, low energy consumption, mobile management, high-speed backhaul, low cost and so on. Information and communications technology (ICT) takes up a considerable proportion of total energy consumption. For instance, currently, ICT accounts for 5% of the world's CO_2 emissions [4] and this is trending upward. Moreover, telecom infrastructures and devices are responsible for large percentage of the annual average power consumption of ICT and this value is 25% in 2012 [5]. Meanwhile, energy efficiency (EE) is becoming a critical metric in the 5G network due to the economic and environmental concerns [6]. Hence, reducing energy consumption in dense small cell networks (DSCNs) is indispensable and urgent.

Recently, energy-efficient communication in wireless networks has earned tremendous attention. The goals of energy-efficient communication can be mostly divided into two categories: 1) maximizing the EE which is defined as the amount of delivered data per energy consumption and 2) minimizing the total network energy consumption while satisfying the users' rate requirements or other quality of service (QoS) requirements. The state-of-the-art techniques for energy-efficient communication in 5G networks are given in [7].

To achieve the network EE optimization, most of existing works focus on resource allocation. In [8], both network-centric EE and user-centric EE are optimized via power allocation. The two optimization problems are solved with centralized and decentralized algorithms, respectively. In addition, the impact of rate constraints is analyzed. In [9], considering that the downlink transmit power is discrete in actual LTE system, the authors formulate EE maximum problem as a fractional discrete optimization issue and address it by proposing a suboptimal polynomial time algorithm. In this algorithm, base stations (BSs) cooperate with some of their interfering BSs and coordinate their power and user selection to maximize the EE. Multi-objective optimization problems are formulated to jointly maximize the network rate and minimize the power consumption in [10] and [11]. In [10], the multi-objective problem is solved based on sequential quadratic programming (SQP) method. In [11], interference pricing mechanism is introduced and the problem is solved with the method of the Pascoletti and Serafini scalarisation. However, users' rate demands are not considered in the multi-objective problems. Power allocation problem for maximizing heterogeneous network (HetNet) EE is formulated as a two-stage Stackelberg Game where the macrocell base station (MBS) is the follower and SBSs are leaders in [12]. At the same time, interference power threshold of SBSs is set to guarantee their performance. Taking fairness into account, a modified network EE metric is optimized by introducing the weights of users' rates in [13]. Power allocation problem of SBSs is formulated as a non-cooperative game to reduce co-tier interference in [14] and to maximize the network EE in [15]. In [14], subchannels are assigned to macrocell users (MUEs) and small cell users (SUEs) orthogonally to eliminate cross-tier interference and a minimal number of subchannels are allocated to MBS to guarantee QoS of MUEs while increasing the MBS's EE. In [15], remaining subchannels are greedily assigned to users with good channel state if all users' rates demands are satisfied. In [16], power control and user scheduling are jointly considered to maximize the network EE by a mean field approach. The mean field game is also used for solving the downlink power control problem of a DSCN to minimize the cost over a certain period of time in [17]. In [18], taking both the BS circuit and user equipment energy consumption into consideration, the authors jointly optimize the time-slot, frequency and power allocation to maximize the EE.

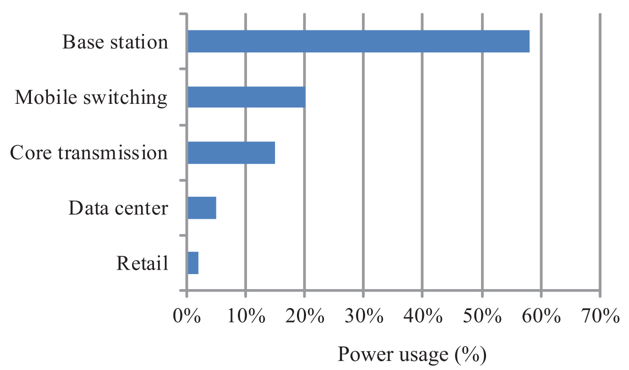

FIGURE 1. **Power consumption of a cellular network (source: Vodafone [19]).**

Fig.1 shows the power consumption of different elements of a cellular network. It can be seen that BSs consume the highest proportion of power. In particular, when BSs are densely deployed, the network energy consumption will tremendously escalate. Therefore, as an efficient approach to minimize energy consumption, sleep mode has been extensively studied. According to the sleep-state duration time of BSs, sleep mode can be classified into coarse time granularity in hours and finer time granularity in milliseconds. In a coarse time granularity, slightly-loaded BSs can be put into sleep mode. However, the coverage hole would arise and the users in the sleeping BSs should attach to other active BSs. In [20] and [21], sleep mode and user association are jointly considered to minimize the power consumption while satisfying users' QoS requirements. In [22], a multi-objective framework is developed to optimize the active sector set and the radio access network (RAN) parameters which aim to minimize the area power consumption and the overlap while maximizing the area SE and the coverage for a given traffic demand density without degrading the QoS. In [23], based on the stochastic geometry model, the influence of the femto BS-sleeping ratio on EE is analyzed and results show that the optimal sleeping ratio is related to both the network traffic load and the location of femtocell deployment area. In a finer granularity of sleep mode, cell discontinuous transmission (DTX) is studied by allowing the transceiver to sleep during the idle time slots for energy saving [24]. References [25] and [26] derive the optimum number of active subframes for transmitting data and BSs can sleep in other subframes to save energy. However, they only consider a single cell network without interference. In addition, resource allocation has also been studied to reduce energy. In [27], the network power minimization is achieved by proposing a pricing-based distributed approach and the rate demands are also considered. Taking both statistical delay constraint and cross-tier interference limit into account, the authors of [28] propose a subchannel and power allocation scheme to reduce power consumption. In addition, several potential energy-saving solutions are defined in 3GPP TR 36.887 (release 12).

Green cellular networks powered by renewable energy can mitigate energy crisis in the future. Therefore, energy harvesting technique has also been investigated to reduce the energy expenditure. In [29], considering BSs with energy harvesting equipment, on-off states of BSs, number of active subchannels and opportunistic sleep time ratio of BSs are jointly optimized to minimize the the average grid power consumption while guaranteeing users' QoS. In the scenario where a macrocell and energy-harvesting small cells are co-channel deployed, the authors derive a power control policy to achieve the target signal-to-interference plus-noise ratio (SINR) of all users taking into account random energy arrivals in [30]. Besides, energy harvesting has also been applied to sustainable wireless sensor networks to prolong the lifetime of nodes [31]. A summary of the approaches for energy-efficient communication discussed in this paper is given in Table 1.

In the previous studies, resource allocation and sleep mode are widely employed to realize green communications.

TABLE 1. Approaches for energy-efficient communication.

Approach	Focus of study	Application scenario	Description
Resource allocation	Power allocation [8–12], [16] and [27], joint power and subchannel allocation [13–15] and [28], joint time-slot, frequency and power allocation [18]	Macrocell networks, DSCNs, massive MIMO network and relay-assisted network	Aim to maximize EE or minimize energy consumption. Low cost, trade-off between performance and energy saving
Sleep mode	BS sleep mode [20–23] and sleep mode in subframes [24] and [25]	Macrocell networks and DSCNs	Aim to minimize energy consumption. Low cost and easy for testing and implementation; save much more energy; coverage hole problem would arise for BS sleep mode
Renewable energy	Energy harvesting [29] and [30]	Macrocell networks and small cell networks	Aim to reduce the energy demand from the power grid. High cost and limited gains

However, they are usually investigated separately and a large number of works ignore the cooperation between BSs. Although BS sleep mode can significantly reduce energy consumption, it would result in coverage hole problem. In this paper, we consider a network architecture where a MBS is always active to provide seamless coverage of control signal and densely deployed SBSs can sleep in some subframes called sleep subframes to save energy. Since SBSs sleep in subframes for only several milliseconds, users in the sleeping SBSs do not need to re-associate to a new SBS for data transmission. Taking advantage of the opportunities of cooperation between SBSs in DSCN, we investigate the energy minimization problem with QoS constraint.

The main contributions of this paper are as follows: (1) SBSs' sleep mode in subframes and power allocation are jointly considered to save energy while satisfying the users' average rate during a frame. This energy-saving problem is formulated as a mixed integer nonlinear programming (MINLP). (2) In order to solve the MINLP problem, we propose a cooperative sleep and power allocation (CSPA) scheme to decompose it into two subproblems where the number of active subframes of SBSs and power allocation are optimized separately. (3) First, we derive the optimum number of active subframes for each SBS in DSCN where co-tier interference exists. Then we develop a centralized heuristic coalition formation algorithm where SBSs cooperate to form coalitions based on the defined coalition formation conditions. (4) SBSs' transmit power in active subframes is optimized to further reduce energy in a distributed way according to a price-based power allocation algorithm.

The rest of the paper is organized as follows. Section II provides the system model and problem formulation. In Section III, the proposed CSPA approach is stated in detail aiming to solve the optimization problem. Performance of the proposed algorithm is evaluated in section IV by system simulation. Finally, Section V concludes the paper.

II. SYSTEM MODEL AND PROBLEM FORMULATION

A. SYSTEM MODEL

We consider a downlink OFDMA network which consists of a macrocell, a local gateway (L-GW) and a large number of small cells deployed within the macrocell area. As shown

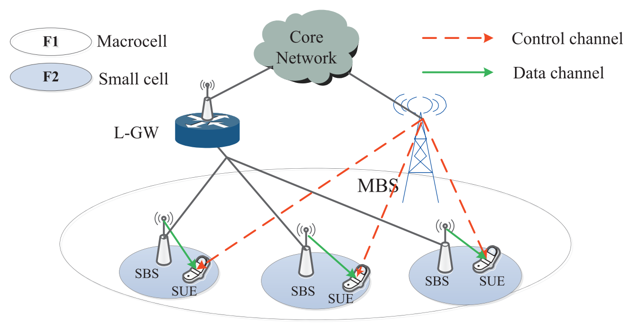

FIGURE 2. Considered network architecture.

in Fig.2, the macrocell is deployed at frequency $F1$ to guarantee coverage and transmit control signal while massive small cells are deployed at frequency $F2$ with universal frequency reuse to improve the hotspots' capacity. So SUEs will not suffer cross-tier interference from the MBS. The macrocell manages the radio resource control (RRC) connection procedures between the user and a small cell such as channel establishment and release. The L-GW provides a medium between small cells and the internet backhaul [32]. All users first get access into macrocells and then receive data service from small cells by the assistance of macrocells.

For each SBS, the total bandwidth B is partitioned into K subchannels, each one with a bandwidth of $B_0 = B/K$ [Hz]. Due to the reuse of subchannels, the co-tier interference will be much severe. In the time domain, each LTE frame consists of N subframes, each one with duration T_{sf}. For simplicity, we assume that each SBS serves only one SUE [33], thus each SUE can be identified by the same label as its serving SBS. Let $\mathcal{M} = \{1, 2, \ldots, M\}$ denote the SBS and SUE set, and $\mathcal{K} = \{1, 2, \ldots, K\}$ denote the subchannel set. Assume that the instantaneous channel state information (CSI) is perfectly known [28] and the channel state remains unchanged during each frame [26]. Thus the upper-bound of the performance can be obtained. Besides, the transmit power of each SBS is assumed to be equally divided among its subchannels. The received SINR of SUE m on subchannel k can be written as

$$\gamma_{mkm} = \frac{p_{mk} h_{mkm}}{\sum\limits_{j=1, j \neq m}^{M} p_{jk} h_{jkm} + \sigma^2} \tag{1}$$

where p_{mk} and p_{jk} denote the transmit power of serving SBS m and interfering SBS j on subchannel k, respectively. h_{mkm} and h_{jkm} are the channel gains from serving SBS m and interfering SBS j to SUE m on subchannel k, respectively. $\sum_{j=1,j\neq m}^{M} p_{jk}h_{jkm}$ denotes the aggregate interference caused by other interfering SBSs to SUE m on subchannel k. σ^2 is the power of additive white Gaussian noise. Therefore, according to Shannon theorem, the amount of delivered data of SUE m on subchannel k in the current frame is expressed as

$$C_{mkm} = \alpha N_{m,act} T_{sf} B_0 \log_2(1+\gamma_{mkm}) \tag{2}$$

where $N_{m,act}$ and α represent the number of active subframes of SBS m for data transmission in a frame and implementation loss, respectively. Thus the average achievable rate of SUE m in SBS m during the current frame is

$$R_{mm} = \frac{1}{NT_{sf}} \sum_{k=1}^{K} C_{mkm} \tag{3}$$

In order to evaluate the power consumption of the DSCN, we use the power model in [34], where the power consumption of SBS m is given by

$$P_{m,total} = \begin{cases} P_0 + \Delta_P \sum_{k=1}^{K} p_{mk} & active \\ P_s & sleeping \end{cases} \tag{4}$$

where Δ_P is a parameter related to the efficiency of the power amplifier and P_0 is the circuit power. P_s is the power consumption of a SBS in sleep mode.

B. PROBLEM FORMULATION

In this paper, SBSs cooperate to form coalitions and SBSs within the same coalition transmit data in time division multiple access (TDMA) way. We desire to minimize the DSCN energy consumption while guaranteeing users' QoS requirements by finding the optimum number of active subframes and power allocation. Therefore, the optimization problem in a frame can be formulated as follows:

$$\min_{\mathbf{N},\mathbf{P}} \sum_{m=1}^{M} T_{sf} \left[N_{m,act} \left(\Delta_P \sum_{k=1}^{K} p_{mk} + P_0 \right) + \left(N - N_{m,act}\right) P_s \right] \tag{5}$$

$$subject\ to: \ C1: R_m \geq R_{m,\min}, \quad \forall m \in \mathcal{M} \tag{6}$$

$$C2: \sum\nolimits_{m \in \mathcal{T}} N_{m,act} \leq N \tag{7}$$

$$C3: 0 \leq p_{mk} \leq P_{mk}^{\max}, \forall m \in \mathcal{M}, \quad \forall k \in \mathcal{K} \tag{8}$$

$$C4: \sum_{k=1}^{K} p_{mk} \leq P_m^{\max}, \quad \forall m \in \mathcal{M} \tag{9}$$

$$C5: N_{m,act} \in \{0, 1, 2, \ldots, N\}, \quad \forall m \in \mathcal{M} \tag{10}$$

where $\mathbf{N} = [N_{1,act} \cdots N_{M,act}]$ and $\mathbf{P} = [\mathbf{P_1} \cdots \mathbf{P_M}]$ are the optimization variables. $\mathbf{P_m}$ denotes the transmit power vector of SBS m over all subchannes, i.e., $\mathbf{P}_m = [p_{m1} \cdots p_{mK}]$ and $R_{m,\min}$ is the target rate of SUE m during a frame. C1 guarantees users' rate requirements. C2 indicates the constraint of total number of active subframes of all SBSs within a coalition and $\mathcal{T}$ denotes a coalition. C3 gives the power constraint on each subchannel and $P_{mk}^{\max}$ is the maximum power that SBS m can radiate on subchannel k. C4 is power allocation constraint of each SBS and $P_m^{\max}$ is the transmit power threshold. C5 represents that the number of active subframes per frame transmission should be an integer between 0 and N. It is noted that the number of active subframes and power allocation are coupled with each other. Therefore, the problem (5)-(10) is a MINLP, which is NP-hard and obtaining its global optimal solution is arduous.

III. COOPERATIVE SLEEP AND POWER ALLOCATION SCHEME

In this section, we propose a CSPA scheme to solve problem (5)-(10) by decomposing it into two subproblems of cooperative sleep (CS) and power allocation. First, the number of active subframes of SBSs is derived. Then, in order to sleep in more subframes, SBSs cooperate to form coalitions via the proposed coalition formation algorithm. Afterwards, to solve the power allocation issue per subframe, a distributed algorithm is developed by introducing interference price.

A. COOPERATIVE SLEEP

Due to dense deployment of SBSs, the co-tier interference is much severe. If SBSs cooperate to form coalitions and SBSs within the same coalitions transmit data in TDMA way and sleep when they do not transmit data, the network power consumption will be reduced. The basic idea of CS is that SBSs serve their users with a minimum number of subframes and sleep in the remaining subframes to save energy via forming coalitions. A coalition $\mathcal{T}_l$ is defined as a non-empty subset of $\mathcal{M}$, and M SBSs in the network are assumed to be partitioned into L disjoint coalitions. A partition of $\mathcal{M}$ is defined as the coalitional structure π_M, i.e., $\pi_M = \{\mathcal{T}_1, \ldots, \mathcal{T}_L\}, \forall i \neq j, \mathcal{T}_i \cap \mathcal{T}_j = \emptyset$, and $\cup_{l=1}^{L} \mathcal{T}_l = \mathcal{M}$. Moreover, considering the network architecture previously mentioned, it is reasonable to let L-GW manage the SBSs to cooperative to form coalitions. This CS scheme includes three parts: interfering SBS matrix construction; active subframe configuration; coalition formation.

1) INTERFERING SBS MATRIX CONSTRUCTION

Although co-tier interference within the same coalition is avoided, the interference from other coalitions still exists. It is assumed that a SUE as a sniffer is located close to the SBS so that each SBS can estimate interference from other SBSs by resorting to the SUE. Note that this SUE is not actual, thus this will not limit the physical location of the SUE in the SBS. For a SBS $m \in \mathcal{T}_i$, since no more than one SBS within a coalition $\mathcal{T}_j, \forall j \neq i$, uses the same subchannel with it per subframe for transmission, there is at most one interfering SBS in coalition $\mathcal{T}_j$ for SBS m. Without loss of generality, we consider the worst condition where the SBS in coalition $\mathcal{T}_j$ causing the most serious interference to SBS m is regarded as the aggressor of SBS m. In order to record the interfering SBSs, we introduce an interfering matrix $A_{M\times M} = \left[a_{mj}\right]_{M\times M}$, where $a_{mj} = 1$ if SBS j is the aggressor of SBS m and $a_{mj} = 0$ otherwise. Note that the elements in the main diagonal are set to be 0, i.e., $a_{mm} = 0$.

2) ACTIVE SUBFRAME CONFIGURATION

According to (1) - (3), it is noted that a user's rate is decided by the number of active subframes of its serving SBS and the transmit power of all SBSs in the network. Therefore, suppose that SBS m has $N_{m,act}$ active subframes during a frame and that the target rate of user m is $R_{m,\min}$, the data rate per active subframe should be achieved to $NR_{m,\min}/N_{m,act}$ such that user's average target rate during a frame can be guaranteed. The needed transmit power of SBS m on subchannel k can be calculated as

$$p_{mk} = \frac{\left(I_{mk}+\sigma^2\right)}{h_{mkm}}\left(2^{\frac{NR_{m,\min}}{\alpha K B_0 T_{sf} N_{m,act}}}-1\right), \quad \forall k\in\mathcal{K} \tag{11}$$

where $I_{mk} = \sum_{j=1,j\neq m}^{M} a_{mj}[k]\,P_{jk}^{\max} h_{jkm}$. Since it is assumed that the power is equal on all subchannels for a SBS, the total transmit power of SBS m is Kp_{mk} in each active subframe. For brevity, we define $\varphi\left(N_{m,act}\right) \triangleq \frac{NR_{m,\min}}{\alpha K B_0 T_{sf} N_{m,act}}$. Substituting (11) into (5) and relaxing $N_{m,act}$ to be a real number with the interval $[0, N]$, the original problem can be converted into:

$$\min_{\mathbf{N}} U(\mathbf{N}) = \sum_{m=1}^{M}\frac{T_{sf}N_{m,act}\Delta_P K\left(I_{mk}+\sigma^2\right)}{h_{mkm}}\left(2^{\varphi(N_{m,act})}-1\right) + \sum_{m=1}^{M} T_{sf}\left[N_{m,act}\left(P_0-P_s\right)+P_s\right] \tag{12}$$

$$\textit{subject to}: \; N_{m,act}\in[0,N], \forall m\in\mathcal{M} \tag{13}$$

The first- and second-order derivative of (12) with respect to $N_{m,act}$ can be calculated as follows:

$$\frac{\partial U(\mathbf{N})}{\partial N_{m,act}} = \frac{T_{sf}\Delta_P K\left(I_{mk}+\sigma^2\right)}{h_{mkm}} \times\left[1-(\ln 2)\,\varphi\left(N_{m,act}\right)\right]2^{\varphi(N_{m,act})} + T_{sf}\left[P_0-P_s-\frac{\Delta_P K\left(I_{mk}+\sigma^2\right)}{h_{mkm}}\right] \tag{14}$$

$$\frac{\partial^2 U(\mathbf{N})}{\partial N_{m,act}^2} = \frac{T_{sf}\Delta_P K\left(I_{mk}+\sigma^2\right)}{h_{mkm}N_{m,act}} \times\left[(\ln 2)\,\varphi\left(N_{m,act}\right)\right]^2 2^{\varphi(N_{m,act})} \geq 0 \tag{15}$$

Therefore, problem (12) is convex in term of $N_{m,act}$. Due to its constraint (13) is also a convex set, the optimal solution $N_{m,act}$ is existent and can be obtained as

$$N_{m,act}^{opt} = \frac{(\ln 2)NR_{m,\min}}{\alpha K B_0 T_{sf}\left[1+lambertw\left(\frac{h_{mkm}(P_0-P_s)}{e(I_{mk}+\sigma^2)K\Delta_P}-\frac{1}{e}\right)\right]} \tag{16}$$

where $lambertw(\cdot)$ is the lambert W-function which is defined as the inverse function of $f(W) = We^W$. The derivation of (16) is in the Appendix. Note that although k is in the right hand of (16), $N_{m,act}^{opt}$ will be the same for any subchannel in SBS m. We use $round(\cdot)$ to obtain the best choice of $N_{m,act}^{opt}$ due to the fact that it should be an integer. From (16), it is noted that larger target rates call for more active subframes. After obtaining the number of active subframes, the location of active subframes should be decided and we call this process active subframe configuration.

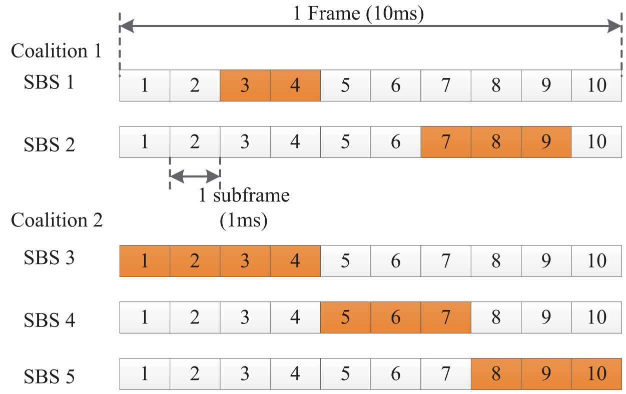

FIGURE 3. **Active subframe configuration.**

Fig.3 shows two cases of active subframe configuration. Each LTE frame is equally divided into 10 subframes, each of which has 1ms in duration. Suppose that SBS 1 and 2 cooperate to form coalition 1 to sleep and that the optimal number of active subframes for SBS 1 and 2 calculated according to (16) are 2 and 3, respectively. So the total active number of subframes in coalition 1 is 5, which is less than 10. L-GW coordinates their active subframe configuration orthogonally, and assigns subframe 3 and 4 to SBS 1 and subframe 7, 8 and 9 to SBS 2, thus they won't introduce interference to the users of each other. In coalition 2, the total number of active subframes is equal to 10. Note that if a SBS m does not cooperate with others, it can configure any $round\left(N_{m,act}^{opt}\right)$ subframes as active subfarmes.

3) COALITION FORMATION

When SBSs form coalitions, they do not transmit data simultaneously, thus the interference introduced to other SBSs outside this coalition can be mitigated. As a result, the needed number of active subframe of SBSs outside this coalition will be reduced and their energy will be saved. Since the purpose of coalition formation is to save the network energy while guaranteeing users' rate requirements, we define the utility of the network as the energy consumption in a frame.

In practice, there are some users whose target rates cannot be achieved, even if their serving SBSs transmit maximum power during the whole frame. This is because their target rates are large and the interference caused by other SBSs is much severe in the DSCNs. We define these users as outage SUEs and others as normal SUEs in this paper.

Accordingly, the outage SUE set is denoted by $\mathcal{M}_{outage}$. We give the coalition formation conditions in definition 1, based on which SBSs can cooperate to form coalitions.

Definition 1: For two given coalitions $\mathcal{T}_i$ and $\mathcal{T}_j$, a new coalition $\{\mathcal{T}_i \cup \mathcal{T}_j\}$ can be formed if the following conditions are satisfied:

$$\{\mathcal{T}_i \cup \mathcal{T}_j\} \triangleright \{\mathcal{T}_i, \mathcal{T}_j\} \Leftrightarrow \begin{cases} \sum_{m\in\{\mathcal{T}_i\cup\mathcal{T}_j\}} N_{m,act} \le N \\ U(\{\mathcal{T}_i \cup \mathcal{T}_j\}) < U(\mathcal{T}_i, \mathcal{T}_j) \\ R_i \ge R_{i,\min}, \forall i \in M \backslash \mathcal{M}_{outage} \end{cases} \tag{17}$$

where $\{\mathcal{T}_i \cup \mathcal{T}_j\} \triangleright \{\mathcal{T}_i, \mathcal{T}_j\}$ means coalition $\mathcal{T}_i$ and coalition $\mathcal{T}_j$ merge into a new coalition $\{\mathcal{T}_i \cup \mathcal{T}_j\}$. $U(\mathcal{T}_i, \mathcal{T}_j)$ and $U(\{\mathcal{T}_i \cup \mathcal{T}_j\})$ denote the utility of the DSCN before and after the new coalition $\{\mathcal{T}_i \cup \mathcal{T}_j\}$ is formed, respectively.

These conditions are as follows: (i) the total number of active subframes per frame in the new coalition should not be more than the number of subframes per frame. (ii) the DSCN energy consumption should be reduced after forming a new coalition; (iii) the target rates of normal users should be achieved when a coalition is formed.

In order to constrain the number of possible partitions, we assume that SBSs maintain their status quo when other SBSs are forming coalitions [35]. According to (17), L-GW can manage SBSs to form coalitions taking into account the system utility and the normal SUEs' rate requirements. Note that if a SBS does not cooperate with others, it will form a coalition alone. The corresponding coalition formation algorithm is described in Algorithm 1 and it includes three stages: initial stage, aggressor discovery stage and coalition merging stage.

Algorithm 1 Coalition Formation Algorithm

- **Initialization**
- Initialize coalition structure in the network as $\mathcal{CS} = \{\{\mathcal{T}_1\}, \ldots, \{\mathcal{T}_M\}\}$. Initialize $p_{mk} = P^{\max}_{mk}, \forall m \in \mathcal{M}, \forall k \in \mathcal{K}$ and the interfering SBS matrix $A_{M\times M}$. Comparing the users' achieved data rate with the rate demands, $\mathcal{M}_{outage}$ is identified.
- **Aggressor discovery**
- **for** SBS $m = 1$ to M **do**
  - Execute *Aggressor discovery* algorithm (Alg. 2).
- **end for**
- L-GW sorts the SBSs in descending order based on their received strongest interference level and maintains them in a victim list $\mathcal{L}_{vim} = \{v1, v2 \ldots, vM\}$.
- **Coalition merging**
- **for** $vi = v1$ to vM **do**
  - Identify the coalition $\mathcal{T}_{vi}$ that SBS vi joins.
  - **repeat**
    - Execute *Coalition merging* algorithm (Alg. 3).
  - **until** $\mathcal{T}_{vi}$ no longer forms a new coalition with its aggressors.
- **end for**

Initially, each SBS forms a coalition alone and serves its user with maximum transmit power. In addition, the interfering SBS matrix $A_{M\times M}$ is initialized. Each SUE compares its actual data rate with its target rate and reports to its serving SBS. Then SBSs inform the L-GW whether its user's rate demand is satisfied such that the outage SUE set can be obtained. Then, each SBS executes the *Aggressor discovery* algorithm (Alg. 2). Once each SBS knows the complete list of aggressors, it informs the L-GW their dominate interference level. After that, L-GW sorts all SBSs in a victim list $\mathcal{L}_{vim} = \{v1, v2 \ldots, vM\}$ in descending order based on the received dominating interference information. The first element $v1$ in the victim list refers to the SBS that suffers the strongest interference level. Finally, SBSs in the network merge into coalitions by executing the *Coalition merging Algorithm* algorithm (Alg. 3). The coalition merging progress continues until the last member vM in $\mathcal{L}_{vim}$ ends its negotiation.

In the aggressor discovery stage, SBS m maintains an aggressor list $\mathcal{L}_{m,\inf} = \{m_1, m_2 \ldots, m_{M-1}\}$ by resorting to its SUE. SBS m_1 in $\mathcal{L}_{m,\inf}$ refer to the SBS causing the most severe interference to SBS m. The aggressor discovery algorithm is shown in Algorithm 2.

Algorithm 2 Aggressor Discovery Algorithm

1. SUE in SBS m measures the received signal strength indicator (RSSI) from other SBSs and reports to SBS m.
2. SBS m sorts its interfering SBSs in descending order and save them in an aggressor list $\mathcal{L}_{m,\inf} = \{m_1, m_2 \ldots, m_{M-1}\}$. The interference level of the strongest aggressor is reported to the L-GW.

In the coalition merging stage, the victims in $\mathcal{L}_{vim}$ begin to merge with their aggressors in its aggressor list from the leading one up to the last one based on the coalition formation conditions. This is due to the fact that SBSs suffering more severe interference are more likely to form coalitions with their aggressors. For the victim vi, it tries to form coalition with its aggressor vi_j in the aggressor list $\mathcal{L}_{vi,\inf}$. Firstly, the coalition ID $\mathcal{T}_{vi}$ which victim vi joins is identified. Secondly, the coalition ID T_{vi_j} which aggressor vi_j joins is identified. Whether $\mathcal{T}_{vi}$ and $\mathcal{T}_{vi_j}$ can form a new coalition $\{\mathcal{T}_{vi} \cup \mathcal{T}_{vi_j}\}$ is determined according to the coalition formation conditions in (17). If (17) is satisfied, the number of active subframes of all SBSs is updated and the subframe configuration is conducted. In addition, the network utility is recorded. The second step is ended if all aggressors in $\mathcal{L}_{vi,\inf}$ are determined. SBSs choose the coalition that can save the most energy to join and remove the member in this coalition from their aggressor lists. The coalition merging algorithm is presented in Algorithm 3.

In order to attain the optimal solution, the possible ways to partition the M elements set are given by the famous Bell Number. However, in our proposed heuristic method, the computational complexity is $O(M^2)$ by using the proposed coalition formation conditions, where M is the total number of SBSs in the network.

Algorithm 3 Coalition Merging Algorithm

for $vi_j = vi_1$ to vi_{M-1} **do**
  Identify the coalition $\mathcal{T}_{vi_j}$ that SBS vi_j joins.
  $\mathcal{T}_{vi}$ tries to form a new coalition $\{\mathcal{T}_{vi} \cup \mathcal{T}_{vi_j}\}$ with $\mathcal{T}_{vi_j}$. Each SBS in the DSCN calculates its number of active subframes according to (16). L-GW determines whether the new coalition can be formed based on (17).
  if (17) is satisfied **then**
    $N^{opt}_{m,act}$ is updated and subframe configuration is conducted. Besides, the current network utility is recorded.
  end if
end for
$\mathcal{T}_{vi}$ merges with the coalition $\mathcal{T}_{vi_j}$ that they can save the most energy if cooperate. Update the interfering SBS matrix $A_{M\times M}$. The members in $\mathcal{T}_{vi}$ remove the elements in $\mathcal{T}_{vi_j}$ from their aggressor lists.

In the coalition formation process, SBSs located close tend to form a coalition. Although the interference between SBSs within a coalition is avoided, the number of active subframes of them is also reduced. Therefore, their users' achieved rates may decrease after forming a coalition. If the normal users' rate demands cannot be met, SBSs will not form coalitions, even if they located close to each other. In such case, the co-tier interference will exist. However, it can be mitigated through power allocation.

B. POWER ALLOCATION

When the number of active subframes of all SBSs and the subframe configuration are known, SBSs can serve users in their active subframes and sleep in the sleeping subframes. In the process of coalition formation, it is assumed that the aggressors transmit with the maximum power, which leads to much energy consumption due to the severe co-tier interference. Consequently, in this subsection, power allocation is optimized to further reduce energy consumption.

A matrix $S_{M\times N} = [s_{mn}]_{M\times N}$ is introduced to indicate the state of a subframe, where $s_{mn} = 1$ if the subframe n of SSB m is active subframe and $s_{mn} = 0$ otherwise. When $S_{M\times N}$ is obtained, the objective function in (5) will become into:

$$\sum_{n=1}^{N} T_{sf} \sum_{m=1}^{M} \left[s_{mn} \left(\Delta_P \sum_{k=1}^{K} p_{mkn} + P_0 \right) + (1 - s_{mn}) P_s \right]$$
$$= \sum_{n=1}^{N} \sum_{m=1}^{M} \left[T_{sf} \Delta_P \sum_{k=1}^{K} s_{mn} p_{mkn} + T_{sf} s_{mn} (P_0 - P_s) + T_{sf} P_s \right] \tag{18}$$

where p_{mkn} denotes the transmit power of SBS m over subchannel k in subframe n. Since T_{sf}, Δ_P, P_0 and P_s are constant and s_{mn} is determinate, the original problem in (5)-(10) can be solved per subframe and it is equivalent to the following problem in subframe n:

$$\min_{\mathbf{P}} \sum_{m=1}^{M} \sum_{k=1}^{K} s_{mn} p_{mkn}$$
$$\textit{subject to}: \; C1, C3, C4 \tag{19}$$

Algorithm 4 Iterative Price-Based Power Allocation Algorithm

Initialize $L_{\max}$ and Lagrangian variables vectors μ and λ. Initialize p_{mkN} with a uniform power distribution $\forall m, k, n$.
for $n = 1$ to N **do**
  Set $l = 0$.
  repeat
    All SBSs calculate the interference price according to (20) and report to their interfering SBSs.
    for $m = 1$ to M **do**
      for $k = 1$ to K **do**
        SBS m updates p_{mk} according to (24)
        μ_m and λ_m are updated according to (25) and (26).
      end for
    end for
    $l = l + 1$
  until Convergence or $l = L_{\max}$
end for

This is a non-convex problem, as the SINRs of SUEs are coupled. Thus finding the global optimal solution is prohibitively complex. In this section, we propose a distributed algorithm (namely, Algorithm 4) to find the local optimal solution of (19) by introducing an interference pricing algorithm. Therefore, (19) can be decomposed into M independent subproblems, one per SBS, by using the pricing interpretation of Karush-Kuhn-Tucker (KKT) conditions [36].

The price of interference that SBS j reports to SBS m over subchannel k in subframe n can be expressed as

$$\pi_{jmn} = -\frac{\partial R_j}{\partial p_{mkn}} = \frac{s_{jn} B_0 p_{jkn} h_{jkj} h_{mkj}}{\ln 2 \left(d_{jkn} + s_{jn} p_{jk} h_{jkj} \right) d_{jkn}} \tag{20}$$

where $d_{jkn} = \sigma^2 + \sum_{m=1, m\neq j}^{M} s_{mn} p_{mkn} h_{mkj}$. Hence, the total interference price received by SBS m in subframe n is

$$u_{mkn} = \sum_{j=1, j\neq m}^{M} \pi_{jmn} \tag{21}$$

In this case, the KKT conditions of (19) are equivalent to the KKT conditions of the following optimization problem, for each SBS m in subframe n:

$$\min_{\mathbf{P_{mn}}} U_{mn} \left(\mathbf{P_{mn}}, \mathbf{P_{-mn}} \right) = \sum_{k=1}^{K} (1 + u_{mkn}) p_{mkn}$$
$$\textit{subject to}: \; C1, C3, C4 \tag{22}$$

where $P_{mn} = [p_{m1n}, p_{m1n}, \ldots, p_{mKn}]$ and $\mathbf{P}_{-\mathbf{mn}} = [p_{11n}, \ldots, p_{1Kn}, \ldots, p_{m-11n}, \ldots, p_{m-1Kn}, p_{m+11n}, \ldots, p_{m+1Kn}]$ are the power vector of SBS m and other SBSs across all subchanels in subframe n, respectively. To find the solution of (19) in a distributed manner, each SBS needs to solve (22) assuming that the interference price is fixed. The problem (22) and its constraints are all convex. Therefore, it is possible to obtain an optimal solution in closed form. The Lagrangian function of (22) is given by

$$\begin{aligned} L(\mathbf{P_{mn}}, \mathbf{P_{-mn}}) &= \sum_{k=1}^{K}(1+u_{mkn})p_{mkn} - \lambda_{mn}\left(P_m^{\max} - \sum_{k=1}^{K}p_{mkn}\right) \\ &\quad -\mu_{mn}\left[\sum_{k=1}^{K}B_0\log_2(1+p_{mkn}\gamma_{mk}) - R_{m,\min}\right] \end{aligned} \tag{23}$$

where $\mu_m n$ and $\lambda_m n$ are the Lagrange multipliers for SBS m in subframe n. By setting $\partial L(\mathbf{P_{mn}}, \mathbf{P_{-mn}}) / \partial p_{mkn} = 0$, the optimal power allocation is derived

$$p_{mkn} = \left[\frac{B_0\mu_{mn}}{\ln 2(1+u_{mkn}+\lambda_{mn})} - \frac{\sigma^2 + \sum\limits_{j=1, j\neq m}^{M} p_{jkn}h_{jkm}}{h_{mkm}}\right]_0^{p_{mk}^{\max}} \tag{24}$$

Based on the subgradient method, the Lagrange multipliers are updated according to the following expressions

$$\begin{aligned} \mu_{mn}^{(l+1)} &= \Bigg\{\mu_{mn} + \xi_{\mu n}^{(l)} \\ &\quad \times \left[R_{m,\min} - \sum_{k=1}^{K}B_0\log_2(1+p_{mkn}\gamma_{mkn})\right]\Bigg\}^{+} \end{aligned} \tag{25}$$

$$\lambda_{mn}^{(l+1)} = \left[\lambda_{mn}^{(l)} + \xi_{\lambda n}^{(l)} \times \left(\sum_{k=1}^{K}p_{mkn} - P_m^{\max}\right)\right]^{+} \tag{26}$$

where $(x)^+ = \max\{x, 0\}$. $\xi_{\mu n}^{(l)}$ and $\xi_{\lambda n}^{(l)}$ are the step sizes of iteration $l \in \{1, 2, \ldots, L_{\max}\}$ in subframe n, $L_{\max}$ is the maximum number of iterations. The proposed price-based power allocation algorithm is shown in Algorithm 4.

In this paper, we assume that only one user exists per small cell. However, the proposed CSPA scheme can be extended to multi-user scenario. In such case, the subframe configurations for users in the same SBS are the same. The main difference is that subchannel allocation among users in the same SBS should be taken into account in the multi-user scenario. The interference between users in the same SBS does not exist in the multi-user scenario since they are allocated to orthogonal subchannels. In addition, it should be noted that the cell size will affect the EE performance. This is due to the fact that the interfering SBS matrix is constructed by resorting to a SUE located close to the SBS and we assume that all users in a SBS have the same interfering SBSs. If the cell size is large, users are randomly located within this area thus the actual interfering SBSs of them may be different. Therefore, the performance will be degraded if their interfering SBSs are still assumed to be the same.

IV. SIMULATION RESULTS AND DISCUSSION

In this section, the system level numerical simulation is developed via Monte-Carlo methods to estimate the performance of the CSPA scheme. For the simulation, we consider the downlink of the OFDMA system and a $100 \times 100\ m^2$ square area with M randomly deployed SBSs within a macrocell. Large scale channel fading is considered, which includes the path-loss and shadow fading. The simulation parameters of system configurations mostly refer to [37]. In particular, main simulation parameters are listed in Table 2.

TABLE 2. Simulation parameters.

Parameter	Value
Carrier frequency $F1/F2$	2.0 GHz/3.5 GHz
System bandwidth	10 MHz
Number of subchannels	10
Number of subframes per frame	10
Subframe duration T_{sf}	1ms
Noise power spectral density	−174dBm/Hz
Small cell path loss model	$140.7 + 36.7\log 10(d[\text{km}])$dB
Traffic model	Full Buffer
Scheduler	Round Robin
Transmit power of MBS/SBS	46 dBm/30dBm
Power consumption $\Delta_P/P_0/P_s$[34]	4.0/6.8W/4.3W
Maximum number of iterations $L_{\max}$	100

We compare CSPA scheme with the maximum power allocation (MPA), the non-cooperative power allocation (NCPA) and the CS schemes. Note that in MPA, all SBSs transmit maximum power over all subchannels during the whole frame. In NCPA, SBSs don't form coalitions and only conduct power allocation using Algorithm 4. In CS, SBSs only form coalitions using Algorithm 1 and transmit maximum power in their active subframes. In the following simulations, we shown the performance of the proposed CSPA scheme with different network densities. Moreover, from (17), we know that the rate requirements can affect coalition formation, thus the impact of target rate is also evaluated.

In Fig. 4, we present a snapshot of a coalitional structure resulting from the proposed coalition formation algorithm with 10 SBSs when the users' average target rates are 5Mbps. Initially, all SBSs schedule their transmissions in non-cooperative way and the total number of coalitions in the DSCNs is 10. After using the proposed algorithm, they form 6 coalitions. In non-cooperative way, SBS 4 suffers the most severe interference. Therefore, in the proposed approach, it forms Coalition 1 with SBS 0 firstly as the coalition formation conditions are satisfied. Following the same reason, SBS 2, 5 and 9 form Coalition 3 and SBS 6 and 7 form Coalition 5, respectively. SBS 1, 3, 8 do not cooperate with others and

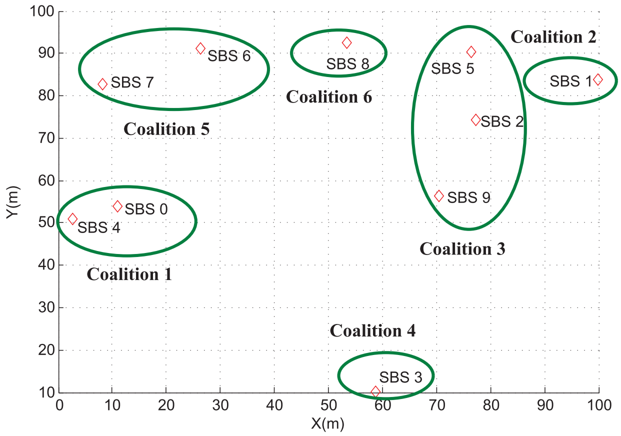

FIGURE 4. A snapshot of a coalitional structure resulting from the proposed approach.

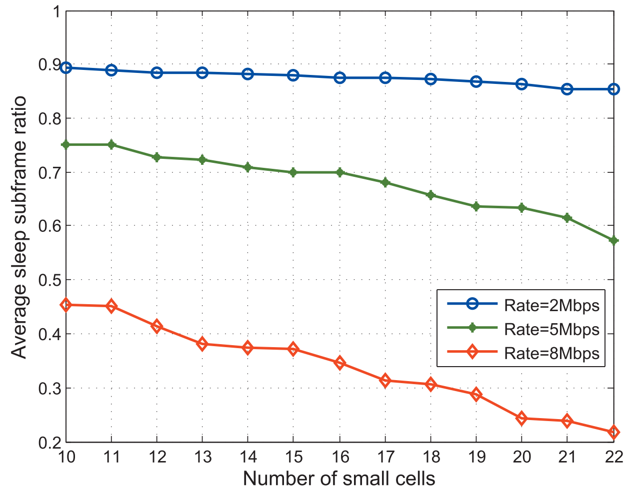

FIGURE 6. Average sleep subframe ratio versus network density.

form coalitions alone. Results suggest that SBSs located close to each other tend to form coalitions to coordinate their transmission due to the severe interference.

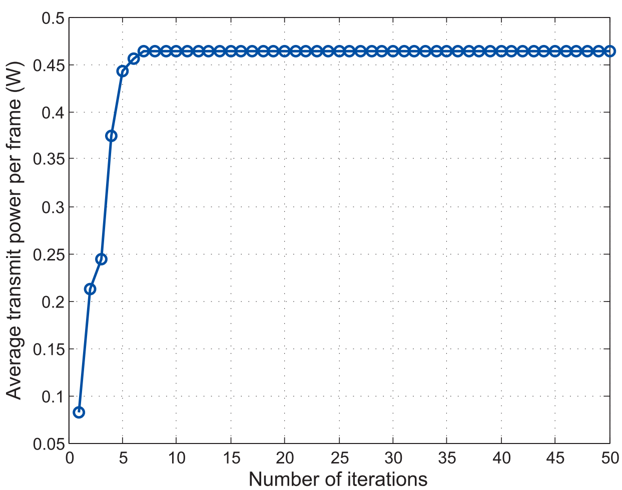

FIGURE 5. Convergence of the proposed Algorithm 2.

In Fig.5, the convergence of Algorithm 4 is evaluated when the users' target rate is 5 Mbps and the number of SBSs is 15. As can be seen from Fig. 5, the average transmit power per frame converges after 10 iterations. This result indicates that the convergence of Algorithm 4 is guaranteed.

Fig.6 shows the average sleep subframe ratio of CSPA with different user's target rates as network density varies. The average sleep subfame ratio is defined as the percentage of the total number of sleep subframes of all SBSs in the DSCN. In the simulation, we select $R_{m,\min} = 2, 5, 8 Mbps$ to respectively represent the low, middle and high rate requirement in a cell. It can be seen that the sleep subframe ratio are more than 80% and less than 50% when the target rates are 2Mbps and 8Mbps, respectively. This is because SBSs need more active subrames to meet their users' larger rate demands. In addition, the average sleep subframe ratio decreases as the network density increases for all target rates due to the fact that more severe interference calls for more active subframes. In particular, the fluctuation of the sleep subframe ratio is shown to be more obvious at larger target rate when the number of SBSs changes from 10 to 22.

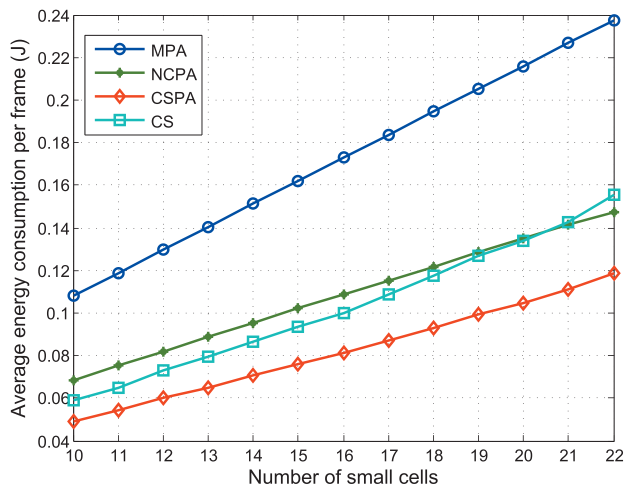

FIGURE 7. Average energy consumption per frame versus network density.

Fig.7 shows the DSCN energy consumption per frame of different schemes versus the network density when the user's target rate is 5 Mbps. It is observed that energy consumption increases with the network density for all schemes and our proposed CSPA scheme can significantly reduce the energy consumption, indicating that cooperation between SBSs is beneficial to energy saving. On the other hand, when the network density is low, CS can save more energy than NCPA since some SBSs turn into sleep mode in the CS scheme. However, when the number of SBSs is more than 20, cooperative sleep is less efficient than power allocation. This is because the number of sleep subframes decreases and SBSs transmit maximum power in their active subframes.

Since there are outage SUEs in the network and coalition formation process in the proposed CSPA scheme can ensure

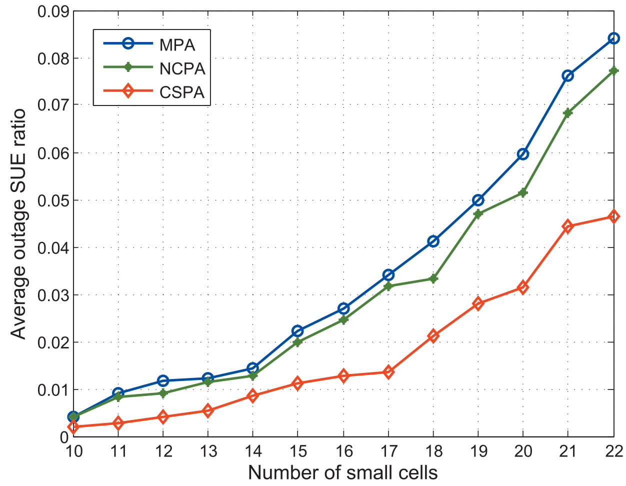

FIGURE 8. **Average outage SUE ratio versus network density.**

less outage SUEs, the average outage SUE ratio with respect to network density is demonstrated in Fig.8. In the simulation, the users' rate demands are assumed to be 5Mbps. The average outage SUE ratio is defined as the percentage of outage SUEs in the DSCN. We can see that the outage SUE ratio increases with the network density. The reason is that given the rate requirement, SBSs need more active subframes to serve users due to the more severe co-tier interference resulting from more SBSs, and some SUEs' target rates can not be satisfied. Obviously, CSPA has a lower outage SUE ratio than NCPA and MPA. This is because in CSPA, some SBSs cooperate to sleep in several subframes thus the interference is mitigated and the target rates are more likely to be achieved.

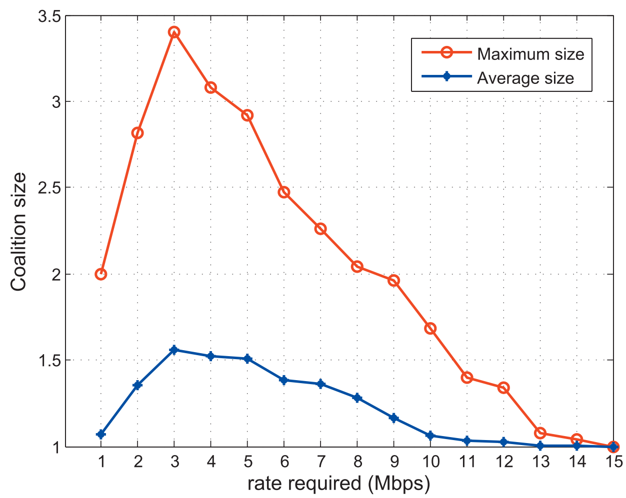

FIGURE 9. **Coalition size versus rate demands.**

The average and maximum sizes of the coalition with respect to rate demand are shown in Fig.9. In this simulation, the total number of SBSs is 15. Since the coalition size is averaged over many independent network realizations, its value is fractional. It can be seen that both the average coalition size and the maximum size first increase then decrease with the target rate. Such phenomena are due to the fact that when two SBSs form coalitions, all SBSs calculate their needed number of active subframes according to (16) and they only need one active subframes to guarantee users' rate requirements when the rate demand is 1Mbps. In this case, cooperation between other SBSs is not needed. With the rate demand growing, SBSs in the network need more active subframes to serve their users and they can form more and larger coalitions to cooperate to sleep in more sleep subframes. However, when the rate demand is larger than 3Mbps and continues to increase, the maximum coalition size and average coalition size decrease. This is because all SBSs need large number of subframes and the coalition formation conditions will not be satisfied. It can be observed that both the maximum and average sizes of coalition are equal to 1 at the rate of 15Mbps, which means that SBSs in the network do not cooperate in this case.

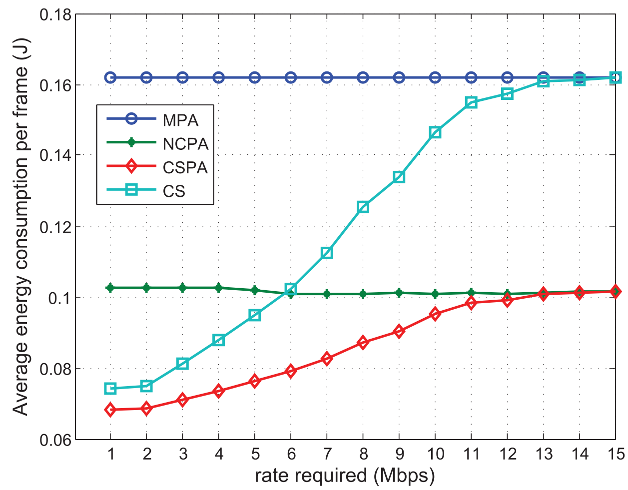

FIGURE 10. **Average energy consumption per frame versus rate demands.**

Fig.10 manifests the DSCN energy consumption per frame as target rate varies when the number of SBSs is 15. It is obvious that the energy consumption is constant in MPA since all SBSs transmit the maximum power during the whole frame regardless of the rate requirements. In NCPA, the energy consumption changes slightly since the circuit dissipation is the major part of energy consumption. When the rate demand is above 6.0Mbps, the CS consumes more energy than NCPA, which implies that conducting power allocation is beneficial to energy saving under large rate requirement. The reason is that SBSs transmit maximum power in more afig3ctive subframes as the target rate grows in CS. However, our proposed CSPA scheme consumes the least energy by jointly considering sleep mode and power allocation. Additionally, we can see that the gap between CSPA and NCPA becomes smaller when rate requirement grows. This is because the number of active subframes increases with the target rate. Similar reason is for MPA and CS schemes. When the rate demand reaches to 15Mbps, the gaps are zero due to the fact that SBSs do not cooperate.

V. CONCLUSION

In this paper, considering the actual frame structure and the cooperation between SBSs in DSCN, we formulate the energy-saving problem with QoS constraint as a MINLP by integrating both sleep mode and power allocation. A CSPA scheme is proposed to solve this problem by decomposing it into two subproblems of cooperative sleep and power allocation. Firstly, we figure out the explicit expression of the optimum number of active subframes for SBSs and give the coalition formation conditions, based on which a centralized heuristic coalition formation algorithm is proposed for SBSs to form coalitions. Subsequently, the power allocation problem is addressed in a distributed way by introducing interference price. Finally, we compare the CSPA scheme with NCPA scheme and MPA scheme. Numerical results demonstrate that given the rate demand, the cooperation between SBSs can lead to more energy savings and meet users' target rates as much as possible when the network density grows. Moreover, given the number of SBSs in the network, their is a rate demand at which SBSs can form the largest coalition. Besides, SBSs will not cooperate when the target rate reaches to a certain value.

In order to solve the spectrum scarcity problem in the 5G network, cognitive radio (CR) communication has been considered as a potential candidate. CR technology has many applications [38] and a novel classification of white spaces is proposed in [39] to promote the development of CR communication. In [40], the authors investigate the resource allocation problem for multiuser OFDMA-based CR networks (CRNs). Cognitive capability is essential for small cells to improve the EE of the small cell tier and solve the interference problem in the HetNets. In the future, we will enhance our work by considering small cells with cognitive radio capability. And the EE optimization problem will be addressed in the scenario where a large number of cognitive small cells and multiple marocells are co-channel deployed.

VI. APPENDIX

PROOF OF OPTIMAL NUMBER OF ACTIVE SUBFRAMES

By setting $\partial U(\mathbf{N}) / \partial N_{m,act} = 0$, we obtain

$$2^{\varphi(N_{m,act})}\left[(\ln 2)\,\varphi\left(N_{m,act}\right)-1\right]=\frac{h_{mk}\left(P_0-P_s\right)}{\Delta_P K\left(I_{mk}+\sigma^2\right)}-1 \tag{27}$$

Using $2^x = e^{x\ln 2}$, $x > 0$, (27) can be expressed as

$$e^{(\ln 2)\varphi(N_{m,act})}\left[(\ln 2)\,\varphi\left(N_{m,act}\right)-1\right]=\frac{h_{mk}\left(P_0-P_s\right)}{\Delta_P K\left(I_{mk}+\sigma^2\right)}-1 \tag{28}$$

Changing the left side of (28) into the formation of We^W, we have

$$\begin{aligned} &e^{(\ln 2)\varphi(N_{m,act})-1}\left[(\ln 2)\,\varphi\left(N_{m,act}\right)-1\right]\\ &=\frac{1}{e}\left[\frac{h_{mk}\left(P_0-P_s\right)}{\Delta_P K\left(I_{mk}+\sigma^2\right)}-1\right] \end{aligned} \tag{29}$$

According to the definition of lambert W-function, (29) becomes

$$(\ln 2)\,\varphi\left(N_{m,act}\right)-1=lambertw\left(\frac{h_{mk}(P_0-P_s)}{e(I_{mk}+\sigma^2)K\Delta_P}-\frac{1}{e}\right) \tag{30}$$

Substituting $\varphi\left(N_{m,act}\right)=\frac{NR_{m,\min}}{\alpha K B_0 T_{sf} N_{m,act}}$ into (30), (16) is derived.

REFERENCES

[1] *Cisco Visual Networking Index: Global Mobile Data Traffic Forecast Update, 2015–2020 White Paper*, document 1454457600805266, Cisco, San Jose, CA, USA, Feb. 2016. [Online]. Available: http://www.cisco.com/c/en/us/solutions/collateral/service-provider/visual-networking-index-vni/mobile-white-paper-c11-520862.pdf

[2] S. Chen and J. Zhao, "The requirements, challenges, and technologies for 5G of terrestrial mobile telecommunication," *IEEE Commun. Mag.*, vol. 52, no. 5, pp. 36–43, May 2014.

[3] N. Bhushan *et al.*, "Network densification: The dominant theme for wireless evolution into 5G," *IEEE Commun. Mag.*, vol. 52, no. 2, pp. 82–89, Feb. 2014.

[4] A. Fehske, G. Fettweis, J. Malmodin, and G. Biczok, "The global footprint of mobile communications: The ecological and economic perspective," *IEEE Commun. Mag.*, vol. 49, no. 8, pp. 55–62, Aug. 2011.

[5] M. Webb *et al.*, "SMART 2020: Enabling the low carbon economy in the information age," *Climate Group. London*, vol. 1, no. 1, p. 1, 2008.

[6] H. Park and T. Hwang, "Energy-efficient power control of cognitive femto users for 5G communications," *IEEE J. Sel. Areas Commun.*, vol. 34, no. 4, pp. 772–785, Apr. 2016.

[7] S. Buzzi, C.-L. I, T. E. Klein, H. V. Poor, C. Yang, and A. Zappone, "A survey of energy-efficient techniques for 5G networks and challenges ahead," *IEEE J. Sel. Areas Commun.*, vol. 34, no. 4, pp. 697–709, Apr. 2016.

[8] A. Zappone, L. Sanguinetti, G. Bacci, E. Jorswieck, and M. Debbah, "Energy-efficient power control: A look at 5G wireless technologies," *IEEE Trans. Signal Process.*, vol. 64, no. 7, pp. 1668–1683, Apr. 2016.

[9] H.-H. Nguyen and W.-J. Hwang, "Distributed scheduling and discrete power control for energy efficiency in multi-cell networks," *IEEE Commun. Lett.*, vol. 19, no. 12, pp. 2198–2201, Dec. 2015.

[10] M. R. Mili, K. A. Hamdi, F. Marvasti, and M. Bennis, "Joint optimization for optimal power allocation in OFDMA femtocell networks," *IEEE Commun. Lett.*, vol. 20, no. 1, pp. 133–136, Jan. 2016.

[11] Z. Fei, C. Xing, N. Li, and J. Kuang, "Adaptive multiobjective optimisation for energy efficient interference coordination in multicell networks," *IET Commun.*, vol. 8, no. 8, pp. 1374–1383, May 2014.

[12] Y. Wang, X. Wang, and L. Wang, "Low-complexity stackelberg game approach for energy-efficient resource allocation in heterogeneous networks," *IEEE Commun. Lett.*, vol. 18, no. 11, pp. 2011–2014, Nov. 2014.

[13] S. Bu and F. R. Yu, "Distributed energy-efficient resource allocation with fairness in wireless multicell OFDMA networks," in *Proc. IEEE Global Commun. Conf.*, Dec. 2014, pp. 4708–4713.

[14] A. Y. Al-Zahrani and F. R. Yu, "An energy-efficient resource allocation and interference management scheme in green heterogeneous networks using game theory," *IEEE Trans. Veh. Technol.*, vol. 18, no. 7, pp. 5384–5396, Jul. 2016.

[15] M. Wang, H. Tian, and G. Nie, "Energy efficient power and subchannel allocation in dense OFDMA small cell networks," in *Proc. IEEE 80th Veh. Technol. Conf. (VTC-Fall)*, Sep. 2014, pp. 1–5.

[16] S. Samarakoon, M. Bennis, W. Saad, M. Debbah, and M. Latva-Aho, "Energy-efficient resource management in ultra dense small cell networks: A mean-field approach," in *Proc. IEEE Global Commun. Conf. (GLOBECOM)*, Dec. 2015, pp. 1–6.

[17] P. Semasinghe and E. Hossain, "Downlink power control in self-organizing dense small cells underlaying macrocells: A mean field game," *IEEE Trans. Mobile Comput.*, vol. 15, no. 2, pp. 350–363, Feb. 2016.

[18] Q. Xu, X. Li, H. Ji, and X. Du, "Energy-efficient resource allocation for heterogeneous services in OFDMA downlink networks: Systematic perspective," *IEEE Trans. Veh. Technol.*, vol. 63, no. 5, pp. 2071–2082, Jun. 2014.

[19] C. Han *et al.*, "Green radio: Radio techniques to enable energy-efficient wireless networks," *IEEE Commun. Mag.*, vol. 49, no. 6, pp. 46–54, Jun. 2011.
[20] Q. Wang and J. Zheng, "A distributed base station on/off control mechanism for energy efficiency of small cell networks," in *Proc. IEEE Int. Conf. Commun. (ICC)*, Jun. 2015, pp. 3317–3322.
[21] P. Piunti, C. Cavdar, S. Morosi, K. E. Teka, E. Del Re, and J. Zander, "Energy efficient adaptive cellular network configuration with QoS guarantee," in *Proc. IEEE Int. Conf. Commun. (ICC)*, Jun. 2015, pp. 68–73.
[22] P. Chandhar and S. S. Das, "Multi-objective framework for dynamic optimization of OFDMA cellular systems," *IEEE Access*, vol. 4, pp. 1889–1914, 2016.
[23] J. Kim, W. S. Jeon, and D. G. Jeong, "Effect of base station-sleeping ratio on energy efficiency in densely deployed femtocell networks," *IEEE Commun. Lett.*, vol. 19, no. 4, pp. 641–644, Apr. 2015.
[24] P. Frenger, P. Moberg, J. Malmodin, Y. Jading, and I. Gódor, "Reducing energy consumption in LTE with cell DTX," in *Proc. IEEE 73rd Veh. Technol. Conf. (VTC Spring)*, May 2011, pp. 1–5.
[25] R. Wang, J. S. Thompson, H. Haas, and P. M. Grant, "Sleep mode design for green base stations," *IET Commun.*, vol. 5, no. 18, pp. 2606–2616, 2011.
[26] H. B. Ren, M. Zhao, J. K. Zhu, and W. Y. Zhou, "Energy-efficient resource allocation for OFDMA networks with sleep mode," *Electron. Lett.*, vol. 49, no. 2, pp. 111–113, Jan. 2013.
[27] F. Ahmed, A. A. Dowhuszko, O. Tirkkonen, and R. Berry, "A distributed algorithm for network power minimization in multicarrier systems," in *Proc. IEEE 24th Annu. Int. Symp. Pers., Indoor, Mobile Radio Commun. (PIMRC)*, Sep. 2013, pp. 1914–1918.
[28] W. Jing, Z. Lu, H. Zhang, Z. Zhang, J. Zhao, and X. Wen, "Energy-saving resource allocation scheme with QoS provisioning in OFDMA femtocell networks," in *Proc. IEEE Int. Conf. Commun. Workshops (ICC)*, Jun. 2014, pp. 912–917.
[29] J. Gong, J. S. Thompson, S. Zhou, and Z. Niu, "Base station sleeping and resource allocation in renewable energy powered cellular networks," *IEEE Trans. Commun.*, vol. 62, no. 11, pp. 3801–3813, Nov. 2014.
[30] T. K. Thuc, E. Hossain, and H. Tabassum, "Downlink power control in two-tier cellular networks with energy-harvesting small cells as stochastic games," *IEEE Trans. Commun.*, vol. 63, no. 12, pp. 5267–5282, Dec. 2015.
[31] F. Akhtar and M. H. Rehmani, "Energy replenishment using renewable and traditional energy resources for sustainable wireless sensor networks: A review," *Renew. Sustain. Energy Rev.*, vol. 45, pp. 769–784, May 2014.
[32] E. Pateromichelakis, M. Shariat, A. Quddus, M. Dianati, and R. Tafazolli, "Dynamic clustering framework for multi-cell scheduling in dense small cell networks," *IEEE Commun. Lett.*, vol. 17, no. 9, pp. 1802–1805, Sep. 2013.
[33] G. Nie, H. Tian, J. Ren, J. Wang, L. Liu, and H. Jiang, "Cooperative power control in OFDMA small cell networks," *EURASIP J. Wireless Commun. Netw.*, vol. 2015, no. 1, pp. 1–17, 2015.
[34] G. Auer *et al.*, "How much energy is needed to run a wireless network?" *IEEE Trans. Wireless Commun.*, vol. 18, no. 5, pp. 40–49, Oct. 2011.
[35] Y. Shi, G. Zhu, S. Lin, J. Ding, and S. Xu, "Coalitional game theory for cooperative interference management in femtocell networks," *Math. Problems Eng.*, vol. 2015, Jun. 2015, Art. no. 767649.
[36] F. Wang, M. Krunz, and S. Cui, "Price-based spectrum management in cognitive radio networks," *IEEE J. Sel. Topics Signal Process.*, vol. 2, no. 1, pp. 74–87, Feb. 2008.
[37] 3GPP, "Technical specification group radio access network; evolved universal terrestrial radio access (E-UTRA); further advancements for E-UTRA physical layer aspects," 3rd Generation Partnership Project (3GPP), Sophia Antipolis Valbonne, France, Tech.Rep. TR36.814 v9.0.0, Mar. 2010
[38] S. H. R. Bukhari, M. H. Rehmani, and S. Siraj, "A survey of channel bonding for wireless networks and guidelines of channel bonding for futuristic cognitive radio sensor networks," *IEEE Commun. Surveys Tuts.*, vol. 18, no. 2, pp. 924–948, 2nd Quart., 2016.
[39] F. Akhtar, M. H. Rehmani, and M. Reisslein, "White space: Definitional perspectives and their role in exploiting spectrum opportunities," *Telecommun. Policy*, vol. 40, no. 4, pp. 319–331, 2016.
[40] K. G. M. Thilina, E. Hossain, and M. Moghadari, "Cellular OFDMA cognitive radio networks: Generalized spectral footprint minimization," *IEEE Trans. Veh. Technol.*, vol. 64, no. 7, pp. 3190–3204, Jul. 2015.

SHIE WU received the B.S. degree in electronic and information engineering from Yantai University, Yantai, China, in 2010, and the M.S. degree in electronic and communication engineering from the Beijing University of Posts and Telecommunication (BUPT), Beijing, China, in 2013. She is currently pursuing the Ph.D. degree in information and communication engineering with BUPT. Her current research interests are in the areas of wireless communications and networks, with an emphasis on resource allocation techniques for energy efficiency in dense small cell networks.

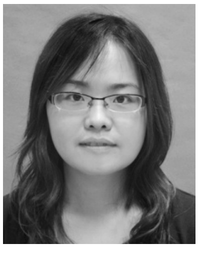

FANGFANG LIU (M'12) received the B.S. and Ph.D. degrees from the Beijing University of Posts and Telecommunication (BUPT), Beijing, China, in 2006 and 2012, respectively. She is currently an Assistant Professor with the School of Information and Communication Engineering, BUPT. Her research interests are in the areas of green wireless communications, 5G cellular networks, and polarization signal processing.

ZHIMIN ZENG received the B.S. degree in carrier communication, the M.S. degree in communication and electronic systems, and the Ph.D. degree in communication and information systems from the Beijing University of Posts and Telecommunication, Beijing, China. He is currently a Professor with the School of Information and Communication Engineering, Beijing University of Posts and Telecommunications. He is a Senior Member of the China Institute of Communications, an Advanced Member of the Chinese Institute of Electronics, and a member of the Academic Committee, BUPT. His current research interests include theory and technology of next generation mobile and wireless networks.

HAILUN XIA (M'13) received the B.Eng. and Ph.D. degrees in wireless telecommunications from the Beijing University of Posts and Telecommunications (BUPT) in 2002 and 2007, respectively. He is currently an Associate Professor with the School of Information and Communication Engineering, BUPT, China. His research field is in the areas of next generation wireless networks with particular focus on dense small cell networks and distributed wireless networks.